# Laminar Segregation of GABAergic Neurons in the Avian Nucleus Isthmi Pars Magnocellularis: A Retrograde Tracer and Comparative Study

Macarena Faunes,[1,2]* Sara Fernández,[1] Cristián Gutiérrez-Ibáñez,[3] Andrew N. Iwaniuk,[4] Douglas R. Wylie,[3] Jorge Mpodozis,[1] Harvey J. Karten,[5] and Gonzalo Marín[1,6]

[1]Departamento de Biología, Facultad de Ciencias, Universidad de Chile, 7800003, Santiago, Chile
[2]Centro de Investigaciones Médicas, Escuela de Medicina, Pontificia Universidad Católica de Chile, 8330023, Santiago, Chile
[3]University Centre for Neuroscience, University of Alberta, Edmonton, Alberta, T6G 2E9, Canada
[4]Department of Neuroscience, Canadian Centre for Behavioural Neuroscience, University of Lethbridge, Lethbridge, Alberta, T1K 3M4, Canada
[5]Department of Neurosciences, School of Medicine, University of California, San Diego, La Jolla, California 92093-0608, United States of America
[6]Facultad de Medicina, Universidad Finis Terrae, 7501015, Santiago, Chile

## ABSTRACT

The isthmic complex is part of a visual midbrain circuit thought to be involved in stimulus selection and spatial attention. In birds, this circuit is composed of the nuclei isthmi pars magnocellularis (Imc), pars parvocellularis (Ipc), and pars semilunaris (SLu), all of them reciprocally connected to the ipsilateral optic tectum (TeO). The Imc conveys heterotopic inhibition to the TeO, Ipc, and SLu via widespread γ-aminobutyric acid (GABA)ergic axons that allow global competitive interactions among simultaneous sensory inputs. Anatomical studies in the chick have described a cytoarchitectonically uniform Imc nucleus containing two intermingled cell types: one projecting to the Ipc and SLu and the other to the TeO. Here we report that in passerine species, the Imc is segregated into an internal division displaying larger, sparsely distributed cells, and an external division displaying smaller, more densely packed cells. In vivo and in vitro injections of neural tracers in the TeO and the Ipc of the zebra finch demonstrated that neurons from the external and internal subdivisions project to the Ipc and the TeO, respectively, indicating that each Imc subdivision contains one of the two cell types hodologically defined in the chick. In an extensive survey across avian orders, we found that, in addition to passerines, only species of Piciformes and Rallidae exhibited a segregated Imc, whereas all other groups exhibited a uniform Imc. These results offer a comparative basis to investigate the functional role played by each Imc neural type in the competitive interactions mediated by this nucleus. J. Comp. Neurol. 521:1727–1742, 2013.



**INDEXING TERMS:** nucleus isthmi; optic tectum; stimulus selection; GABAergic; hodological homology; parcellation

## INTRODUCTION

The vertebrate isthmic complex (parabigeminal nucleus in mammals) is a heterogeneous neural assemblage providing visual feedback to the optic tectum (TeO; superficial portion of the superior colliculus in mammals). In birds, the isthmic complex is composed of the nuclei isthmi pars magnocellularis (Imc), isthmi pars parvocellularis (Ipc), and isthmi pars semilunaris (SLu). Each of these nuclei receives a topographic visual projection from the "shepherd-crook" neurons located in tectal layer 10 (Wang et al., 2004, 2006). Ipc and SLu neurons are choline acetyl transferase immunopositive (ChAT+; Medina and Reiner, 1994; Wang et al., 2006) and project back to the TeO in a precisely homotopic fashion (Hunt et al., 1977; Güntürkün and Remy, 1990; Wang et al., 2006). Imc neurons are γ-aminobutyric acid (GABA) and glutamic



Grant sponsor: Chilean National Science and Technology Research Fund (FONDECYT); Grant numbers: 1080220 and 1110281 (to G.M.); Grant sponsor: Natural Sciences and Engineering Research Council (NSERC); Grant number: Discovery G121210071 (to D.R.W.).

*CORRESPONDENCE TO: Macarena Faunes, Departamento de Anatomía Normal, Escuela de Medicina, Pontificia Universidad Católica de Chile, Lira 44, 8330023 Santiago, Santiago de Chile. E-mail: macare.fc@gmail.com

Received August 2, 2012; Revised October 9, 2012; Accepted October 25, 2012
DOI 10.1002/cne.23253
Published online November 1, 2012 in Wiley Online Library (wileyonlinelibrary.com)

acid decarboxylase (GAD) immunopositive (GABA+, GAD+; Braun et al., 1988; Domenici et al., 1988; Tömböl and Németh, 1998; Sun et al., 2005) and send wide terminal fields extending throughout the Ipc, the SLu, and the deep layers of the TeO (Wang et al., 2004).

The isthmotectal network has recently emerged as a model of competitive stimulus selection and visual spatial attention in several species of vertebrates (Sereno and Ulinski, 1987; Marín et al., 2005, 2007, 2012; Gruberg et al., 2006; Asadollahi et al., 2010, 2011; Mysore et al., 2010, 2011; Knudsen, 2011). Two main observations support these roles. First, feedback signals provided by the Ipc boost the propagation of retinal visual inputs from the TeO to higher visual areas (Marín et al., 2007, 2012). Second, long-range inhibitory interactions focus feedback from the Ipc on those locations in the TeO receiving the strongest visual stimulation (Marín et al., 2007, 2012; Asadollahi et al., 2010, 2011). Therefore, only stronger visual signals are transmitted to higher tectofugal areas. In the pigeon (*Columba livia*), the long-range inhibitory interactions that focus the Ipc feedback upon the tectal visual map depend on Imc activity, stressing the role of this nucleus in the stimulus selection process (Marín et al., 2007).

In the chick (*Gallus gallus*), in which the anatomical organization of the isthmotectal circuit has been thoroughly described, intracellular filling of Imc neurons revealed two neuronal subtypes: Imc-Is neurons, projecting to both the Ipc and SLu, and Imc-Te neurons, projecting only to the TeO (Wang et al., 2004). Individual neurons projecting to both the Ipc/SLu and the TeO were not found (Wang et al., 2004). Each Imc-Te neuron extends an axonal arborization over wide areas in the deep layers of the TeO, with the exception of the tectal region providing the neuron's own visual input. This organization has been referred to as antitopographic (Wang et al., 2004; Lai et al., 2011) and supports a possible "winner-take-all" function.

Because both Imc neuronal types are found intermingled within the nucleus in chicks (Wang et al., 2004), it has been difficult to differentially label, record, or pharmacologically manipulate their activity. Thus, the specific roles played by the two different Imc neural types within their respective targets are unknown. Moreover, it is not clear whether the projection of the Imc-Is to the Ipc and SLu is also antitopographic, or whether each neural type differs in its visual tectal afferents.

In addition to the chick (Wang et al., 2004, 2006; Meyer et al., 2008; Shao et al., 2009; Lai et al., 2012), the avian isthmotectal network has been intensively studied in the pigeon (Hunt et al., 1977; Güntürkün and Remy, 1990; Marín et al., 2005, 2007, 2012), and the barn owl (*Tyto alba*, Maczko et al., 2006, Mysore et al., 2010; Asadollahi et al., 2011; Knudsen, 2011). In both species, the Imc also exhibits a uniform cytoarchitectonic appearance (Mikula et al., 2007). In the zebra finch (*Taeniopygia guttata*), however, an early report showed that the Imc is segregated into two easily distinguishable GABA+ subdivisions referred to as the dorsal and ventral Imc (Braun et al., 1988). Because of this segregation, songbirds could prove to be a useful model within which to investigate the differential roles of these two cell types in the Imc.

In this study, we characterize the anatomical organization of the Imc in the zebra finch, seeking to determine whether the two subdivisions of this nucleus correspond to an anatomical segregation of the two hodologically defined cell types in the chick. We also made an extensive survey across avian orders to assess whether the segregated Imc is a specific feature of passerines or it is shared by other avian groups.

## MATERIALS AND METHODS

Injections of neural tracers and experimental procedures were performed on 20 adult male and female zebra finches (*Taeniopygia guttata*) and three chicks of undetermined sex (*Gallus gallus*) purchased from a local dealer. For the comparative survey across avian orders, we analyzed 40-μm-thick, thionin- and cresyl violet-stained sections of the mesencephalon of one specimen of each of the 99 species listed in Tables 1 and 2. These specimens were adults from either sex, obtained from the collections of avian brains from the laboratory at the University of Alberta of D.W. and A.I. ($n = 88$), the laboratory at the University of California San Diego of H.J.K. ($n = 1$), and the laboratory at the Universidad de Chile of G.M. and J.M ($n = 10$). All procedures used in this study were approved by the bioethics committee of the Facultad de Ciencias of the Universidad de Chile and conformed to U.S. National Institutes of Health guidelines for the use of animals in experimental research.

### Histology

Experimental animals were anesthetized with a mixture of 50 mg/kg ketamine and 20 mg/kg xylazine, and perfused transcardially with 0.75% saline, followed by chilled 4% paraformaldehyde (PFA) in 0.1 M phosphate-buffered saline (PBS; 0.75% NaCl; pH 7.2–7.4). The brains were removed from the skull and postfixed overnight in the PFA/PBS solution. They were then transferred to 30% sucrose in 0.1 M phosphate buffer (PB) until they sank, and cut coronally at 50 or 60 μm on a freezing sliding microtome. Three series of sections were collected in PBS. Sections from one series were Nissl-stained (cresyl violet; Merck, Darmstadt, Germany) and used for histological analysis.

TABLE 1.
Passerine Species Used in This Study

| Species | Common name | Family |
|---|---|---|
| *Gymnorhina tibicen* | Australian magpie | Artamidae |
| *Bombycilla cedrorum* | Cedar waxwing | Bombycillidae |
| *Cormobates leucophaea* | White-throated treecreeper | Climacteridae |
| *Zonotrichia capensis* | Rufous-collared sparrow | Emberizidae |
| *Emblema pictum* | Painted firetail | Estrildidae |
| *Stagonopleura guttata* | Diamond firetail | Estrildidae |
| *Taeniopygia guttata* | Zebra finch | Estrildidae |
| *Taeniopygia bichenovii* | Owl finch | Estrildidae |
| *Euphagus carolinus* | Rusty blackbird | Icteridae |
| *Acanthorhynchus tenuirostris* | Eastern spinebill | Meliphagidae |
| *Lichenostomus penicillatus* | White-plumed honeyeater | Meliphagidae |
| *Manorina melanocephala* | Noisy miner | Meliphagidae |
| *Menura novaehollandiae* | Superb lyrebird | Menuridae |
| *Grallina cyanoleuca* | Magpie-lark | Monarchidae |
| *Acanthiza pusilla* | Brown thornbill | Pardalotidae |
| *Pardalotus punctatus* | Spotted pardalote | Pardalotidae |
| *Poecile atricapillus* | Black-capped chickadee | Paridae |
| *Erythrura gouldiae* | Gouldian finch | Passeridae |
| *Eopsaltria australis* | Eastern yellow robin | Petroicidae |
| *Petroica multicolor* | Pacific robin | Petroicidae |
| *Sturnus vulgaris* | Common starling | Sturnidae |
| *Turdus merula* | Common blackbird | Turdidae |
| *Turdus falcklandii* | Austral thrush | Turdidae |
| *Elaenia albiceps* | White-crested elaenia | Tyrannidae |

## Estimation of cell size, total cell number, and nucleus volume in the Imc

Using the Nissl-stained sections, contours of the Imc were traced in a Nikon Eclipse E400 microscope equipped with an x-y-z motor stage and the Stereo Investigator software (MBF Bioscience, Williston, VT). Contours were used to estimate the nuclear volumes according to the Cavalieri principle and to generate 3D reconstructions. Cell number estimates were obtained by using a 100× immersion-oil objective and the optical fractionator probe provided by the Stereo Investigator software. Nucleoli were counted in counting frames of 80 × 80 μm long and 15 μm high distributed over the Imc by using a Systematic Random Sampling grid. The grid size was varied to reach a Gundersen error coefficient (CE) $\leq$ 0.1. Guard zones of at least 2 μm were used. For cell size estimation, the long diameter of neuronal profiles at the focal plane of the nucleolus was measured in each counting frame.

## Analysis of the Imc across several avian species

For the comparative survey across species, photomicrographs of coronal Nissl-stained sections containing the Imc nucleus were examined by three investigators, who classified the Imc of each specimen as "segregated" or "uniform" without knowing the species identity. Imc was classified as "segregated" when an internal, less dense cell division could be readily separated from an external, more densely packed cell division. A classification was accepted when two of the three raters agreed. However, for the majority of specimens (95 out of 99), all three raters agreed.

## Tracer crystal deposits in vitro

The preparation of slices of the mesencephalon was as described by Wang et al. (2004). Briefly, 13 adult male zebra finches were anesthetized as described above and then decapitated. The brains were quickly removed from the skull and placed in a dish containing chilled, oxygenated, and sucrose-substituted artificial cerebrospinal fluid (ACSF; 240 mM sucrose, 3 mM KCl, 3 mM $MgCl_2$, 23 mM $NaHCO_3$, 1.2 mM $NaH_2PO_4$, 11 mM D-glucose). The midbrain was blocked and sectioned at 500 μm on a vibratome (Campden Vibroslice 752; WPI, Sarasota, FL) in the coronal plane. Slices were collected and submerged in a collecting chamber containing ACSF (119 mM NaCl, 2.5 mM KCl, 1.3 mM $Mg_2SO_4$, 1.0 mM $NaH_2PO_4$, 26.2 mM $NaHCO_3$, 11 mM D-glucose, 2.5 mM $CaCl_2$) at room temperature and continuously oxygenated with a mixture of 95% $O_2$ and 5% $CO_2$.

Prior to injection of the tracers, the slices were transferred to a dish mounted on a zoom stereo microscope (EMZ-TR; Meiji, Santa Clara, CA). The surface of the slice was briefly dried with tissue paper. One or a few penetrations in either the Imc or the Ipc were made by using a tungsten needle whose tip was covered with either biocytin (cat. #B4261; Sigma-Aldrich, St. Louis, MO), rhodamine-conjugated biocytin (cat. #T-12921; Molecular Probes, Eugene, OR), or fluorescein-conjugated biotinylated dextran amine (BDA_ crystals (10,000 molecular weight, cat. #D-7178; Molecular Probes). Then the slices were quickly transferred back to the collecting chamber. Drying and injecting the slice took less than 120 seconds. The slices were kept in oxygenated ACSF for 6 additional hours before fixation. Slices were subsequently fixed by overnight immersion in PFA and then transferred to 30% sucrose in PB until they sank (usually 1 day).

Each slice was frozen and resectioned at 60 μm on the freezing sliding microtome. Sections with biocytin crystal deposits were collected in PBS, kept for 15 minutes in 0.3% hydrogen peroxide in 50% methanol to block endogenous peroxidase activity, and washed again in PBS. Sections were then incubated in avidin-coupled peroxidase solution (ABC kit, Vector, Burlingame, CA) at 4°C overnight. The reaction product was visualized with

TABLE 2.

Non-Passerine Species Examined in This Study

| Species | Common name | Family | Order | Imc nucleus segregated (S)/ uniform (U) |
|---|---|---|---|---|
| *Accipiter cirrocephalus* | Collared sparrowhawk | Accipitridae | Accipitriformes | U |
| *Buteo swainsoni* | Swainson's hawk | Accipitridae | Accipitriformes | U |
| *Anas castanea* | Chestnut teal | Anatidae | Anseriformes | U |
| *Anas superciliosa* | Pacific duck | Anatidae | Anseriformes | U |
| *Chenonetta jubata* | Australian wood duck | Anatidae | Anseriformes | U |
| *Anas crecca carolinensis* | Green-winged teal | Anatidae | Anseriformes | U |
| *Anas clypeata* | Northern shoveler | Anatidae | Anseriformes | U |
| *Anas discors* | Blue-winged teal | Anatidae | Anseriformes | U |
| *Mergus serrator* | Red-breasted merganser | Anatidae | Anseriformes | U |
| *Bucephala clangula* | Common goldeneye | Anatidae | Anseriformes | U |
| *Aythya americana* | Redhead | Anatidae | Anseriformes | U |
| *Aythya affinis* | Lesser scaup | Anatidae | Anseriformes | U |
| *Anas plathyrynchos* | Mallard | Anatidae | Anseriformes | U |
| *Bucephala albeola* | Bufflehead | Anatidae | Anseriformes | U |
| *Calypte anna* | Anna's hummingbird | Trochilidae | Apodiformes | U |
| *Patagona gigas* | Giant hummingbird | Trochilidae | Apodiformes | U |
| *Adelomyia melanogenys* | Speckled hummingbird | Trochilidae | Apodiformes | U |
| *Eutoxeres condamini* | Buff-tailed sicklebill | Trochilidae | Apodiformes | U |
| *Sephanoides sephanoides* | Green-backd firecrown | Trochilidae | Apodiformes | U |
| *Eugenes fulgens* | Magnificent hummingbird | Trochilidae | Apodiformes | U |
| *Glaucis hirsuta* | Rufous-breasted hermit | Trochilidae | Apodiformes | U |
| *Phaethornis superciliosus* | Long-tailed hermit | Trochilidae | Apodiformes | U |
| *Amazilia tzacatl* | Rufous-tailed hummingbird | Trochilidae | Apodiformes | U |
| *Collocalia esculenta* | Glossy swiftlet | Apodidae | Apodifromes | U |
| *Podargus strigoides* | Tawny frogmouth | Podargidae | Caprimulgiformes | U |
| *Eurostopodus argus* | Spotted nightjar | Caprimulgidae | Caprimulgiformes | U |
| *Chroicocephalus philadelphia* | Bonaparte's gull | Laridae | Charadriiformes | U |
| *Chroicocephalus novaehollandiae* | Silver gull | Laridae | Charadriiformes | U |
| *Vanellus chilensis* | Southern lapwing | Charadriidae | Charadriiformes | U |
| *Scolopax rusticola* | Eurasian woodcock | Scolopacidae | Charadriiformes | U |
| *Limnodromus griseus* | Short-billed dowitcher | Scolopacidae | Charadriiformes | U |
| *Phaps elegans* | Brush bronzewing | Columbidae | Columbiformes | U |
| *Streptopelia chinensis* | Spotted dove | Columbidae | Columbiformes | U |
| *Ducula spilorrhoa* | Torresian imperial pigeon | Columbidae | Columbiformes | U |
| *Geopelia humeralis* | Bar-shouldered dove | Columbidae | Columbiformes | U |
| *Columba leucomela* | White-headed pigeon | Columbidae | Columbiformes | U |
| *Geopelia placida* | Peaceful dove | Columbidae | Columbiformes | U |
| *Leucosarcia melanoleuca* | Wonga pigeon | Columbidae | Columbiformes | U |
| *Columba livia* | Pigeon | Columbidae | Columbiformes | U |
| *Ceryle alcyon* | Belted kingfisher | Cerylidae | Coraciiformes | U |
| *Dacelo novaeguineae* | Laughing kookaburra | Halcyonidae | Coraciiformes | U |
| *Falco columbarius* | Merlin | Falconidae | Falconiformes | U |
| *Falcipennis canadensis* | Spruce grouse | Phasianidae | Galliformes | U |
| *Gallus gallus* | Chick | Phasianidae | Galliformes | U |
| *Alectoris chukar* | Chukar | Phasianidae | Galliformes | U |
| *Phasianus colchicus* | Ring-necked pheasant | Phasianidae | Galliformes | U |
| *Perdix perdix* | Gray partridge | Phasianidae | Galliformes | U |
| *Bonasa umbellus* | Ruffed grouse | Phasianidae | Galliformes | U |
| *Nycticorax caledonicus* | Nankeen night heron | Ardeidae | Pelecaniformes | U |
| *Bubulcus ibis* | Cattle egret | Ardeidae | Pelecaniformes | U |
| *Pelecanus conspicillatus* | Australian pelican | Pelecanidae | Pelecaniformes | U |
| *Aulacorhynchus prasinus* | Emerald toucanet | Ramphastidae | Piciformes | S |
| *Indicator variegatus* | Scaly-throated honeyguide | Indicatoridae | Piciformes | S |
| *Pogoniulus bilineatus* | Yellow-rumped tinkerbird | Lybiidae | Piciformes | S |
| *Sphyrapicus varius* | Yellow-bellied sapsucker | Picidae | Piciformes | S |
| *Diomedea* sp. | Albatross | Diomedeidae | Procellariiformes | U |
| *Puffinus tenuirostris* | Short-tailed shearwater | Procellariidae | Procellariiformes | U |
| *Cacatua tenuirostris* | Long-billed corella | Cacatuidae | Psittaciformes | U |
| *Nymphicus hollandicus* | Cockatiel | Cacatuidae | Psittaciformes | U |
| *Cacatua roseicapillus* | Galah | Cacatuidae | Psittaciformes | U |

TABLE 2. (Continued)

| Species | Common name | Family | Order | Imc nucleus segregated (S)/ uniform (U) |
|---|---|---|---|---|
| *Myiopsitta monachus* | Monk parakeet | Psittacidae | Psittaciformes | U |
| *Alisterus scapularis* | Australian king parrot | Psittaculidae | Psittaciformes | U |
| *Glossopsitta porphyrocephala* | Purple-crowned lorikeet | Psittaculidae | Psittaciformes | U |
| *Melopsittacus undulatus* | Budgerigar | Psittaculidae | Psittaciformes | U |
| *Polytelis swainsonii* | Superb parrot | Psittaculidae | Psittaciformes | U |
| *Trichoglossus haematodus* | Rainbow lorikeet | Psittaculidae | Psittaciformes | U |
| *Gallinula tenebrosa* | Dusky moorhen | Rallidae | Gruiformes | S |
| *Fulica americana* | American coot | Rallidae | Gruiformes | S |
| *Aegolius acadicus* | Northern saw-whet owl | Strigidae | Strigiformes | U |
| *Asio flammeus* | Short-eared owl | Strigidae | Strigiformes | U |
| *Bubo virginianus* | Great horned owl | Strigidae | Strigiformes | U |
| *Surnia ulula* | Northern hawk-owl | Strigidae | Strigiformes | U |
| *Tyto alba* | Barn owl | Tytonidae | Strigiformes | U |
| *Nothoprocta perdicaria* | Chilean tinamou | Tinamidae | Tinamiformes | U |

Abbreviation: Imc, isthmi pars magnocellularis.

diaminobenzidine (DAB). Sections were mounted on gelatin-coated slides, counterstained with Nissl, dehydrated, and coverslipped with Entellan mounting medium (Merck). Injection sites and labeled neurons and terminals locations were reconstructed in Neurolucida (MBF Bioscience). Sections with rhodamine-conjugated biocytin and fluorescein-conjugated BDA crystals were collected in PBS, counterstained with 4,6-diamidino-2-phenylindole (DAPI), and then mounted and coverslipped with Vectashield mounting medium (Vector).

### In vivo CTB injections into the TeO

Three adult male zebra finches were anesthetized as described above and placed in a stereotaxic head holder. The skull was exposed and a craniotomy was made dorsal and anterior to the ear canal, above the lateral portion of the TeO. An approximated volume of 500 nL of CTB (1% in PB; cat #104; List, Campbell, CA) was injected by using a Hamilton syringe. These injections were centered approximately in the coordinate 2 mm anterior of the zebra finch stereotaxic atlas of Nixdorf-Bergweiler and Bischof (2007). The syringe was retracted, the wound was closed, and the animal was allowed to recover. After a survival time of 5 days, animals were anesthetized with ketamine and xylazine and perfused with paraformaldehyde solution as described above. The brains were removed from the skull, postfixed, equilibrated in sucrose, and sectioned at 60 μm. Standard immunohistochemistry procedures were applied to reveal cholera toxin B (CTB) distribution. Briefly, sections were incubated with antibodies against CTB made in goat (polyclonal antibody raised in goat against the native purified CTb subunit, 1:12,000; cat. #703; List), followed by biotinylated IgG antibodies (anti-goat IgG, made in rabbit, 1:200; Vector). Avidin-coupled peroxidase (ABC kit, Vector) and DAB were used as the final steps in the visualization of the CTB. Sections were mounted on gelatin-coated slides, counterstained with Nissl, and then dehydrated and coverslipped with Entellan mounting medium (Merck). Injection sites, labeled neurons, and terminal locations were reconstructed by using the Neurolucida software.

### Photomicrograph acquisition and editing

All photomicrographs were taken by using a Spot digital camera (25.4 Mp, Slider, Diagnostic Instruments Inc.) and the Spot Advanced software (Diagnostic Instruments, Arnold, MD). Some of the photomicrographs were converted from color to grayscale, and all of them were adjusted for brightness and contrast by using Photoshop (Adobe Systems, San Jose, CA). The red fluorescence images were converted to magenta by copying the red channel signal to the blue channel.

## RESULTS

### Organization of the Imc nucleus in passerines

It has been reported that in the zebra finch, the Imc appears to be composed of two subdivisions (Braun et al., 1988). We corroborated this finding by examining Nissl-stained coronal sections of zebra finch mesencephalon, in which these subdivisions are readily distinguishable by their clear cytoarchitectonic differences (Fig. 1A–D). Braun et al. (1988) referred to them as dorsal and ventral Imc. However, because at their lateral aspects, the "dorsal" Imc lies medial to the "ventral" Imc throughout the rostrocaudal levels (Fig. 1), we shall instead refer to them as the internal Imc (Imc-in) and external Imc (Imc-ex). The Imc-ex contains smaller and more densely packed cells than the Imc-in. Furthermore, a narrow zone

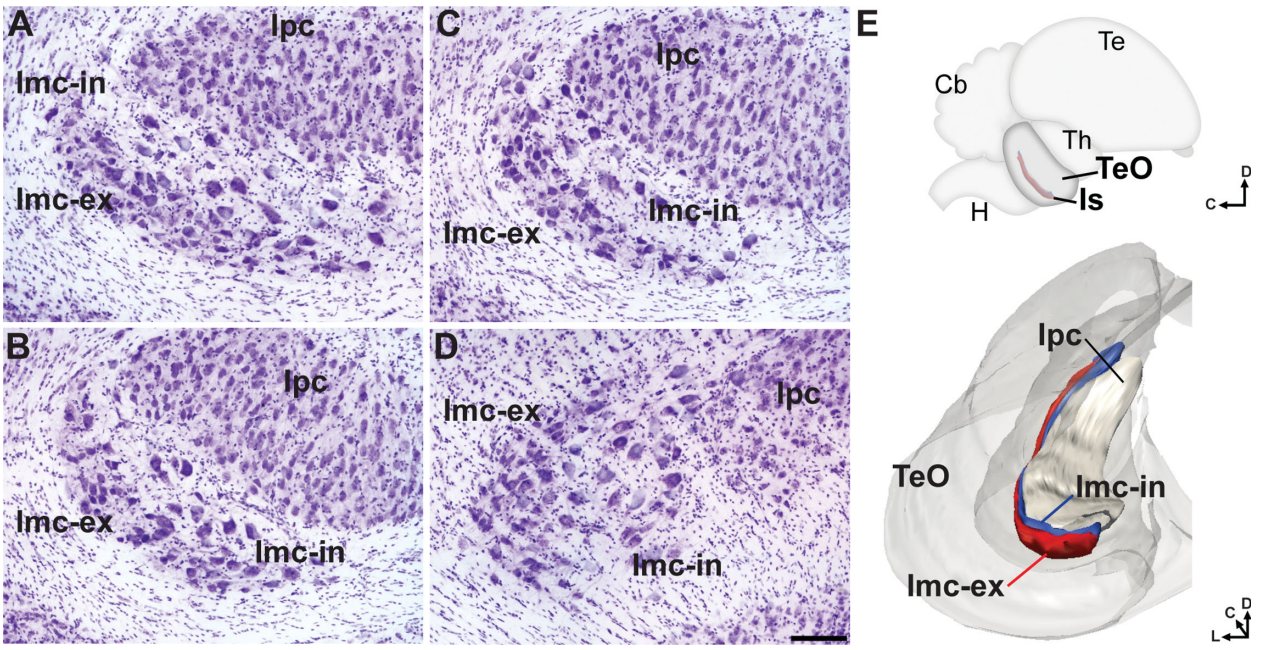


**Figure 1.** The nucleus isthmi magnocellularis (Imc) of the zebra finch (*Taeniopygia guttata*). **A–D**: Brightfield photomicrographs of 60-μm Nissl-stained coronal sections showing the two subdivisions of the Imc, internal (Imc-in) and external (Imc-ex). Sections are separated by 360 μm and displayed from rostral to caudal (midline to the right). Ipc, nucleus isthmi parvocellularis. **E**: Upper image, schematic drawing of a lateral view of the zebra finch brain depicting the position of the isthmic nuclei (upper image). Lower image, Neurolucida reconstruction of an anterior view of the Imc (Imc-in displayed in blue and Imc-ex displayed in red) and the Ipc (displayed in light gray) of the zebra finch. Cb, cerebellum; H, hindbrain; Is, isthmic nuclei; Te, telencephalon; TeO, optic tectum; Th, thalamus; D, dorsal, C, caudal, L, lateral. Scale bar = 50 μm in D (applies to A–E).

devoid of stained somata separates these two regions along the rostrocaudal axis. The 3D reconstruction of the Imc revealed that both subdivisions exhibit a similar extension in the rostrocaudal and dorsoventral axes, appearing as two layers surrounding the lateral aspect of the Ipc (Fig. 1E).

To investigate whether other passerines shared this trait with the zebra finch, we examined the Imc of 23 species of Passeriformes. These species (see Table 1) comprised representatives of 15 oscine families–including the basal family Menuridae (Ericson et al., 2002)–and the suboscine family Tyrannidae. In contrast to the uniform cytoarchitecture of the Imc of the chick (Fig. 2A) and the pigeon (Fig. 2B), in all the passerine species examined (Fig. 2C–E) the Imc nucleus appears clearly subdivided into an Imc-in and an Imc-ex. Thus, the presence of these subdivisions seems to be a common trait of all passerines.

We quantified the cytoarchitectonic differences between the Imc subdivisions by measuring the neuronal size, total cell number, and volume of each subdivision in four passerine species: the zebra finch ($n = 4$, *Taeniopygia guttata*, Estrildidae), the rufous-collared sparrow ($n = 1$, *Zonotrichia capensis*, Emberizidae), the austral thrush ($n = 1$, *Turdus falcklandii*, Turdidae), and the white-crested elaenia ($n = 1$, *Elaenia albiceps*, Tyrannidae). In all examined specimens, the major axis of the Imc-in cells was about 20% larger than that of the Imc-ex cells (in the zebra finch, 27.6 ± 0.45 μm in the Imc-in, and 21.9 ± 0.49 μm in the Imc-ex, mean ± SEM, $n = 4$, paired *t*-test, $P < 0.05$; Table 3). The Cavalieri and optical fractionator methods were used to estimate, respectively, the total volume and total number of cells of the Imc-in and Imc-ex (Table 3). Although the two Imc subdivisions have about the same volume (for the zebra finch 0.15 ± 0,019 $mm^3$ in the Imc-in and 0.167 ± 0.017 $mm^3$ in the Imc-ex, mean ± SEM $n = 4$, paired *t*-test, $P > 0.05$, Table 3), the number of cells and thus the cell density in the Imc-ex is roughly double the number of cells in the Imc-in (for the zebra finch, 1,562 ± 52.5 cells in the Imc-in and 3,547 ± 340.7 cells in the Imc-ex, $n = 4$, paired *t* test, $P < 0.05$; Table 3).

## Retrograde labeling of Imc cells in the zebra finch

To establish whether the cells of the two Imc subdivisions have different projections within the isthmotectal network, we performed in vitro and in vivo injections of neural tracers into the TeO and the Ipc of the zebra finch,

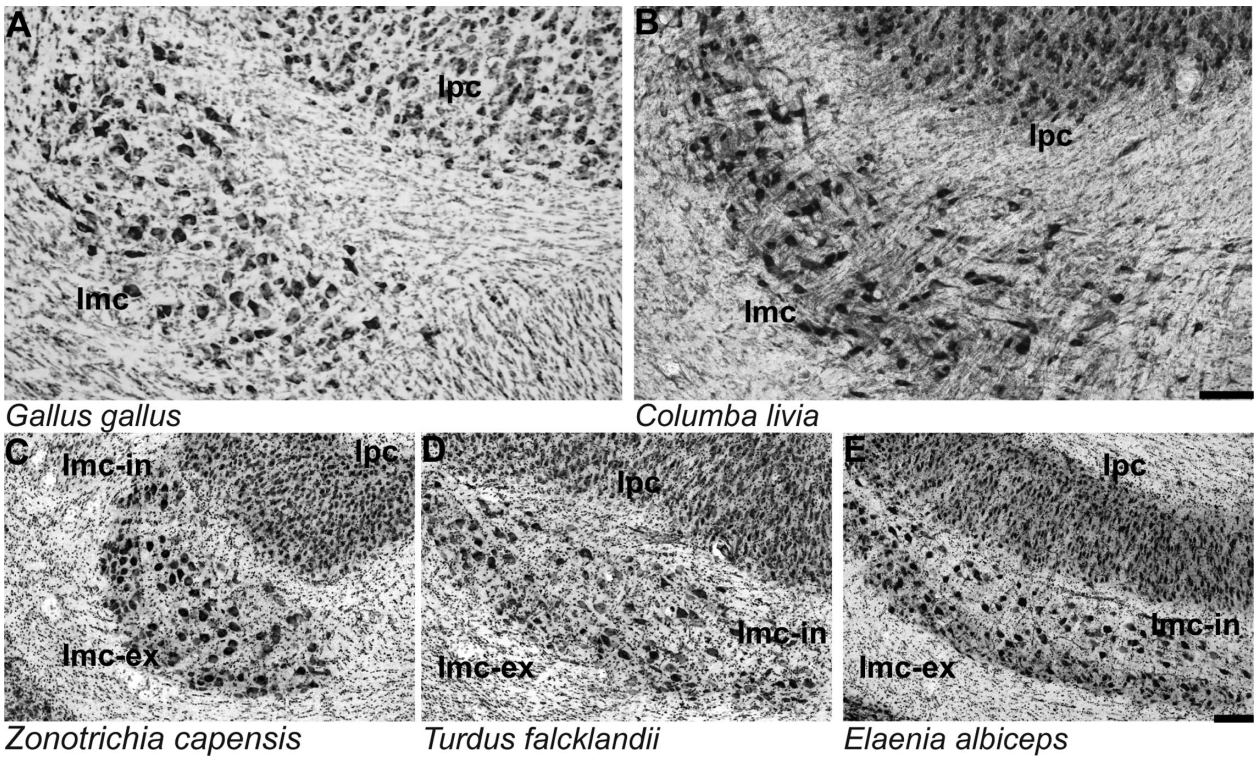


**Figure 2.** Brightfield photomicrographs of 60-μm Nissl-stained coronal sections of the nucleus isthmi magnocellularis (Imc) of non-passerine (A,B) and passerine species (C–E). **A**: The chick, *Gallus gallus*. **B**: The pigeon, *Columba livia*. **C**: The rufous-collared sparrow, *Zonotrichia capensis*. **D**: The austral thrush, *Turdus falcklandii*. **E**: The white-crested elaenia, *Elaenia albiceps*. Midline to the right. For abbreviations, see legend to Figure 1. Scale bar = 100 μm in B (applies to A,B) and E (applies to C–E).

and assessed the resulting pattern of retrograde labeling in the Imc.

Single and double tracer deposits of crystalline tracers into the TeO and the Ipc of zebra finches were performed in 500-μm-thick coronal slice preparations, similar to a preparation previously shown to contain the basic connectivity of the isthmotectal circuit in the chick (Wang et al., 2004, 2006). Following the deposition of biocytin crystals into the TeO, retrogradely labeled cells in the Imc were located almost exclusively in the Imc-in (98.9% of a total of 93 labeled cells in eight slices, five animals; Fig. 3). Labeled axonal terminals from tectal shepherd-crook neurons were evident in both the Imc-in and the Imc-ex, and also in the Ipc and the SLu. As expected, the Ipc exhibited retrogradely labeled somata intermingled with the labeled fibers (Wang et al., 2006).

After biocytin deposits into the Ipc, retrogradely labeled neurons in the Imc were found restricted to the Imc-ex (95.4% of a total of 283 labeled cells in eight slices obtained from five different animals; Fig. 4). Labeled fibers and axonal terminals were found in both the Imc-in and the Imc-ex, and sometimes also in the SLu. The SLu labeling presumably corresponds to axonal collaterals, originating from tectal shepherd-crook neurons projecting to the SLu. In these cases, we also observed retrogradely labeled shepherd-crook neurons in the tectum, and anterogradely labeled paintbrush axons from the Ipc (with their characteristic columnar terminal field; Wang et al., 2006).

Double deposits of retrograde tracers corroborated these findings. After deposits of rhodamine-conjugated biocytin in the Ipc and fluorescein-conjugated BDA in the TeO, red fluorescent-labeled neurons were found in the Imc-ex, whereas green fluorescent-labeled cells were located in the Imc-in (five slices obtained from three different animals; Fig. 5). No double-labeled cells were found. The same experiment in chicken mesencephalon slices also showed no double-labeled cells, and, as expected, fluorescein-labeled cells and rhodamine-labeled cells were found intermingled (data not shown).

In all cases, labeled cells after tracer deposits in the TeO were less frequent than those labeled after tracer deposits in the Ipc (a mean of 11 labeled cells per slice vs. 35 cells per slice), even though the tracer deposits in the first case were about four times larger. This result is in close agreement with previous in vivo results obtained in the chick (Wang et al., 2004).

To rule out the possibility that a presumptive projection from the Imc-ex to the TeO could have been severed in

TABLE 3.

Cell Sizes, Total Cell Numbers, and Volumes of Imc-in and Imc-ex of Four Passerine Species

| | | Imc-in | | | | Imc-ex | | | |
|---|---|---|---|---|---|---|---|---|---|
| Cell size (mean long axis, μm) | | Mean | | SEM[1] | CV | Mean | | SEM[1] | CV |
| | *T. guttata* | 27.6 | | 0.45 | 0.03 | 21.9 | | 0.49 | 0.04 |
| | *T. falcklandii* | 29.0 | | 0.32 | 0.15 | 21.1 | | 0.21 | 0.17 |
| | *Z. capensis* | 27.6 | | 0.33 | 0.19 | 20.1 | | 0.32 | 0.15 |
| | *E. albiceps* | 24.9 | | 0.32 | 0.17 | 21.1 | | 0.30 | 0.17 |
| Total cell no. | | No. | CE[2] | SEM | CV | No. | CE[2] | SEM | CV |
| | *T. guttata* ($n = 4$) | 1,562 | 0.1 | 52.5 | 0.07 | 3,547 | 0.08 | 340.7 | 0.19 |
| | *T. falcklandii* ($n = 1$) | 1,420 | 0.1 | – | | 3,317 | 0.08 | – | |
| | *Z. capensis* ($n = 1$) | 2,710 | 0.08 | – | | 4,280 | 0.08 | – | |
| | *E. albiceps* ($n = 1$) | 1,327 | 0.09 | – | | 1,957 | 0.07 | – | |
| Nucleus volume ($mm^3$) | | Mean | | SEM | CV | Mean | | SEM | CV |
| | *T. guttata* $n = 4$) | 0.150 | | 0.019 | 0.25 | 0.167 | | 0.017 | 0.21 |
| | *T. falcklandii* ($n = 1$) | 0.249 | | – | | 0.357 | | – | |
| | *Z. capensis* ($n = 1$) | 0.220 | | – | | 0.155 | | – | |
| | *E. albiceps* ($n = 1$) | 0.099 | | – | | 0.111 | | – | |
| Cell density (no./$mm^3$)[3] | | | | | | | | | |
| | *T. guttata* | 10,413 | | | | 21,240 | | | |
| | *T. falcklandii* | 5,703 | | | | 9,291 | | | |
| | *Z. capensis* | 12,318 | | | | 27,613 | | | |
| | *E. albiceps* | 13,404 | | | | 17,631 | | | |

[1]$N > 100$ cells (see Materials and Methods); for *T. guttata* the mean between four animals is informed.
[2]C.E. Gundersen (m = 1).
[3]Calculated as the ratio between the estimated cell number and estimated nucleus volume.Abbreviations: Imc-ex, nuclei isthmi pars magnocellularis, external division; Imc-in, Imc, internal division.

our slice preparation, we performed in vivo microinjections of CTB into the TeO of three zebra finches. After a large microinjection (500 nL of 1% CTB, resulting in an injection site with a darkly stained center of approximately 0.1 $mm^3$ surrounded by a less stained region of approximately 0.2 $mm^3$), the retrogradely labeled cells in the Imc (<25 cells in each case) were exclusively located within the Imc-in ($n = 3$; Fig. 6). As in the in vitro experiments, retrogradely labeled cells were also found in the Ipc, and labeled fibers were found in both subdivisions.

## Imc nucleus in other groups of birds

The previously used avian models for the study of the isthmotectal circuit, all of which exhibit a uniform Imc nucleus, belong to three different orders: Galliformes (the chick), Columbiformes (the pigeon), and Strigiformes (the barn owl). To investigate whether the segregated Imc is an exclusive character of Passeriformes, we examined the Imc nucleus in specimens of 73 species pertaining to 16 different orders (Table 2).

Only in Piciformes (woodpeckers, honey-guides, toucans) and Rallidae (rails, order Gruiformes) were we able to detect segregation of the Imc into two discrete components (Fig. 7, Table 2). This was valid for the two examined species of rails (the American coot, *Fulica americana* and the dusky moorhen, *Gallinula tenebrosa*) and the four species from four different families examined in Piciformes (the emerald toucanet, *Aulacorhynchus prasinus*, family Ramphastidae; the Scaly-throated Honeyguide, *Indicator variegatus*, family Indicatoridae; the yellow-rumped tinkerbird, *Pogoniulus bilineatus*, family Lybiidae; and the yellow-bellied sapsucker, Sphyrapicus varius, family Picidae). The remaining 14 orders exhibiting a uniform Imc included the basal groups Tinamiformes, Anseriformes, and Galliformes, suggesting that the ancestral state corresponds to a uniform Imc.

# DISCUSSION

In this study, we found that the presence of two readily distinguishable cytoarchitectonic domains in the Imc nucleus is a common feature among passerines. Our retrograde tracer deposit and microinjection experiments in the zebra finch revealed that the neurons in the Imc-in project to the TeO, whereas the neurons in the Imc-ex project to the Ipc. Moreover, we find that the most common, and presumably the ancestral type of the avian Imc is the uniform type, and that the anatomical segregation

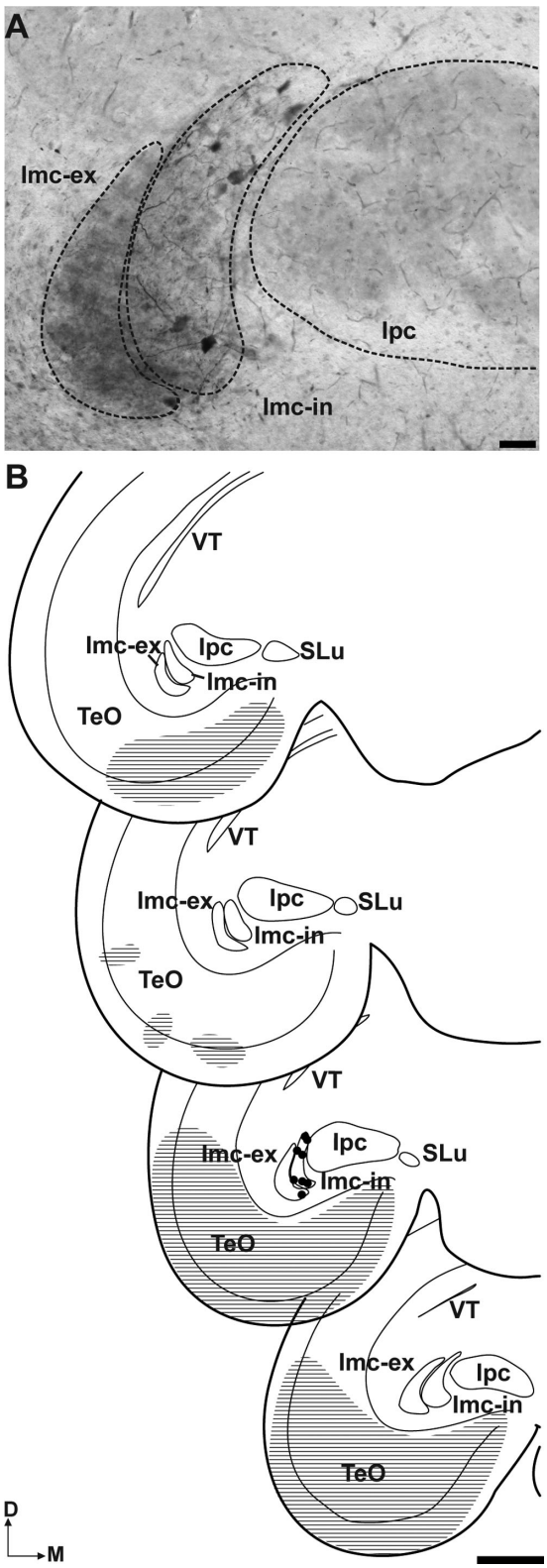


Figure 3. Retrogradely labeled cells in the nucleus isthmi magnocellularis after an in vitro deposit of biocytin crystals in the optic tectum. A: Brightfield photomicrograph of a 60-μm coronal section. Note that the labeled neurons are restricted to the internal layer of the lmc. B:) Line drawings of a series of sections obtained from the same slice. Displayed sections (from rostral to caudal) are separated by 120 μm. Dots represent labeled somata and dark hatched area represents the crystal deposit. SLu, nucleus isthmi pars semilunaris; V, ventricule. For other abbreviations, see legend to Figure 1. Scale bar = 50 μm in A; 500 μm in B.

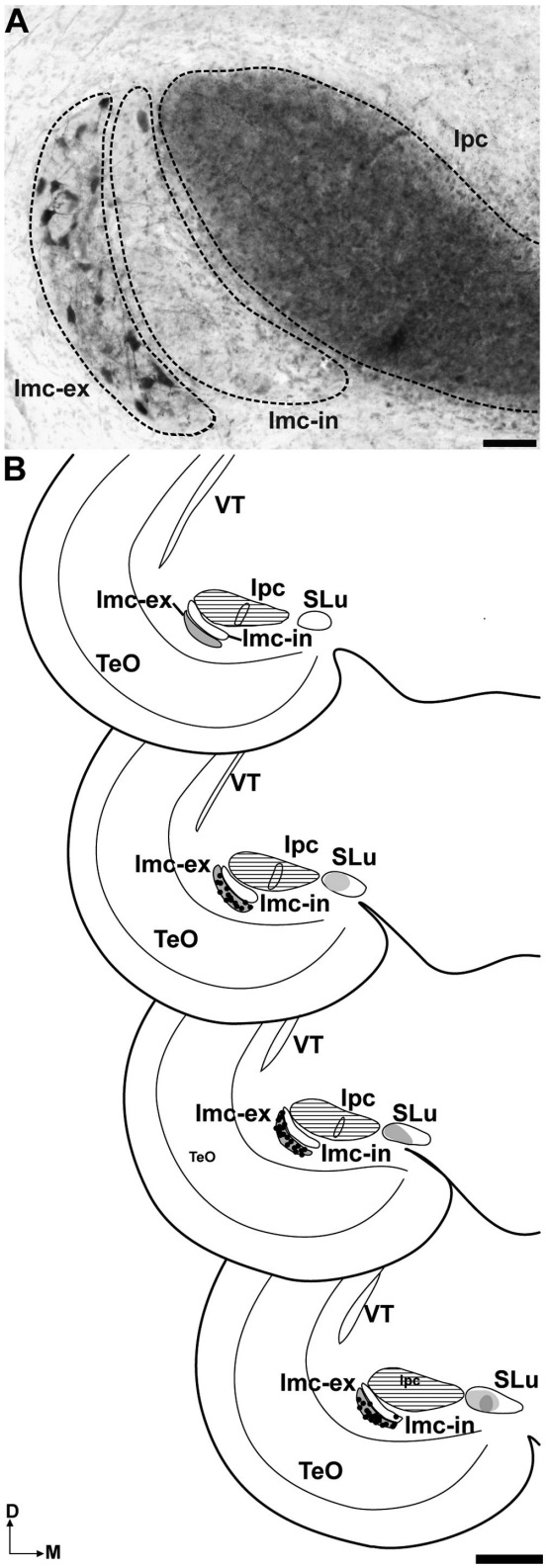


Figure 4. Retrogradely labeled cells in the nucleus isthmi magnocellularis after an in vitro deposit of biocytin crystals in the nucleus isthmi parvocellularis. A: Brightfield photomicrograph of a 60-μm coronal section displaying labeled neurons restricted to the external layer of the lmc. B: Line drawings of a series of sections obtained from the same slice. Displayed sections (from rostral to caudal) are separated by 120 μm. Dots represent labeled somata, hatched area represents the crystal deposit, and light gray shadow represents labeled fibers. For abbreviations, see legend to Figure 1. Scale bar = 50 μm in A; 500 μm in B.

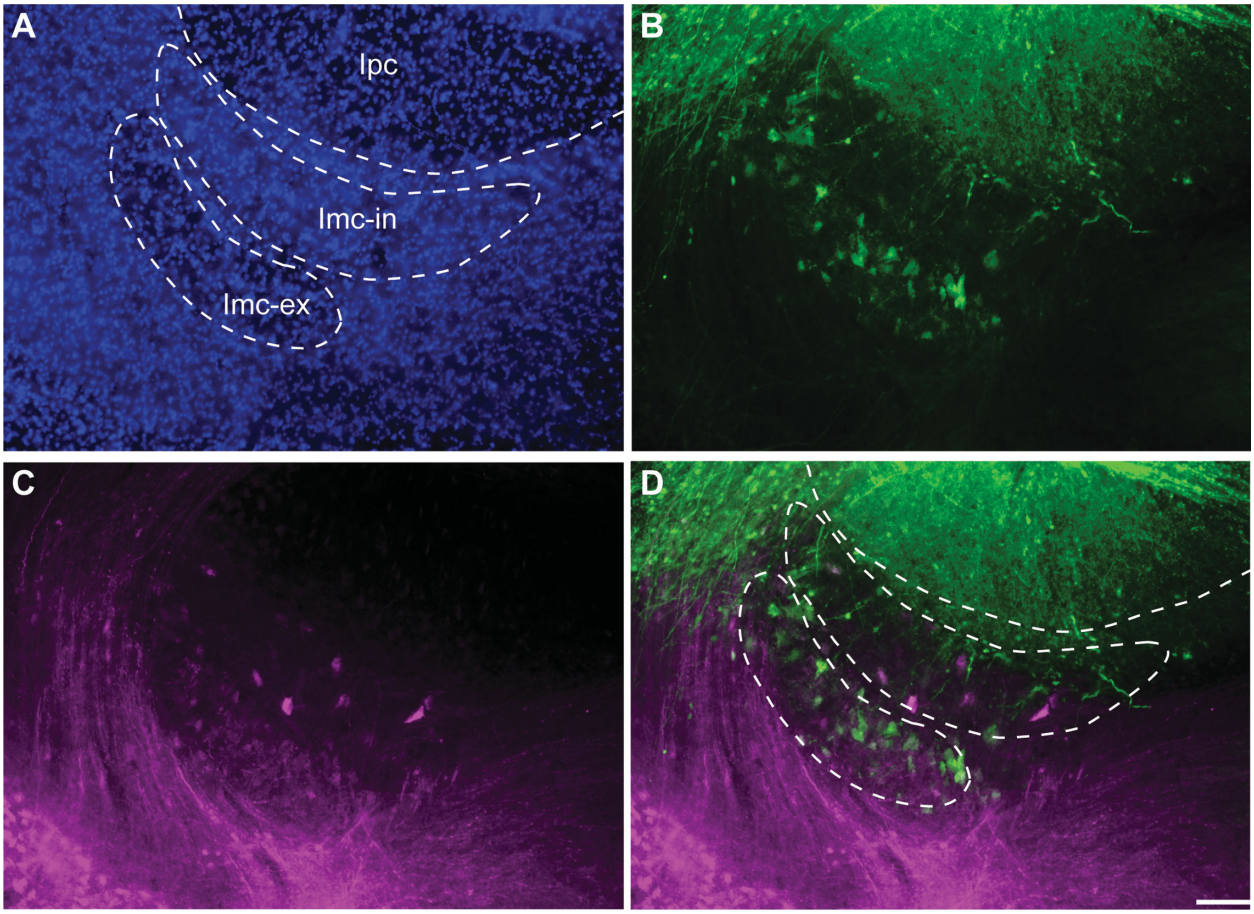


Figure 5. Retrogradely labeled cells after an in vitro double tracer deposit in the nucleus isthmi parvocellularis (fluorescein-conjugated BDA, green) and the optic tectum (rhodamine-conjugated biocytin, magenta) in vitro. A–D: Fluorescence photomicrographs of a 60-μm coronal section containing labeled cells in the nucleus isthmi magnocellularis. **A**: DAPI counterstaining. **B**: Labeling after tracer deposit in the Ipc. **C**: Labeling after deposit in the TeO. **D**: Merged image. For abbreviations, see legend to Figure 1. Scale bar = 50 μm in D (applies to A–D).

of the Imc into the Imc-in and Imc-ex is present in Passeriformes, Piciformes, and Gruiformes.

## The Imc nucleus in Passeriformes

As previously noted by Wang et al. (2004), the Imc of chicks contains two different populations of GABAergic neurons within the boundaries of the Imc. One projects upon the optic tectum, and the other projects upon the Ipc and SLu. The present study revealed that in Passerines these two populations form two readily separable groups, greatly facilitating future studies on the role of each population in visual operations. Wang et al. (2004) referred to these two populations of cells as Imc-Te and Imc-Is. In the present study, we found that Imc-Te cells form a distinct cluster like the Imc-in and the Imc-Is cells form a second cluster as the Imc-ex. These two subdivisions of the Imc nucleus in passerines are organized into two multicellular layers located along the lateral and the posterior aspect of the Ipc nucleus. In all of the passerine species studied, both layers have approximately similar volumes, but the Imc-in contains larger, more sparsely distributed, and thus less numerous cells than the Imc-ex (Table 3). Similarly, in the chick Imc nucleus, there appear to be fewer Imc-Te cells than Imc-Is cells: Of the 46 cells that Wang et al. (2004) filled and fully reconstructed in the chick Imc, 31 projected to the nucleus Ipc and only 15 projected to the TeO. This suggests that the proportional number of cells projecting to the two targets is a conserved trait in the avian isthmotectal circuit.

## Anatomical segregation of the nucleus Imc occurred at least three times in avian evolution

Our observations across several avian species suggest that the presence of a dual population of cells in a seemingly single Imc nucleus is the ancestral state for Neornithes. Besides passerines, bipartite anatomical segregation of the Imc nucleus occurs in Piciformes and Rallidae.

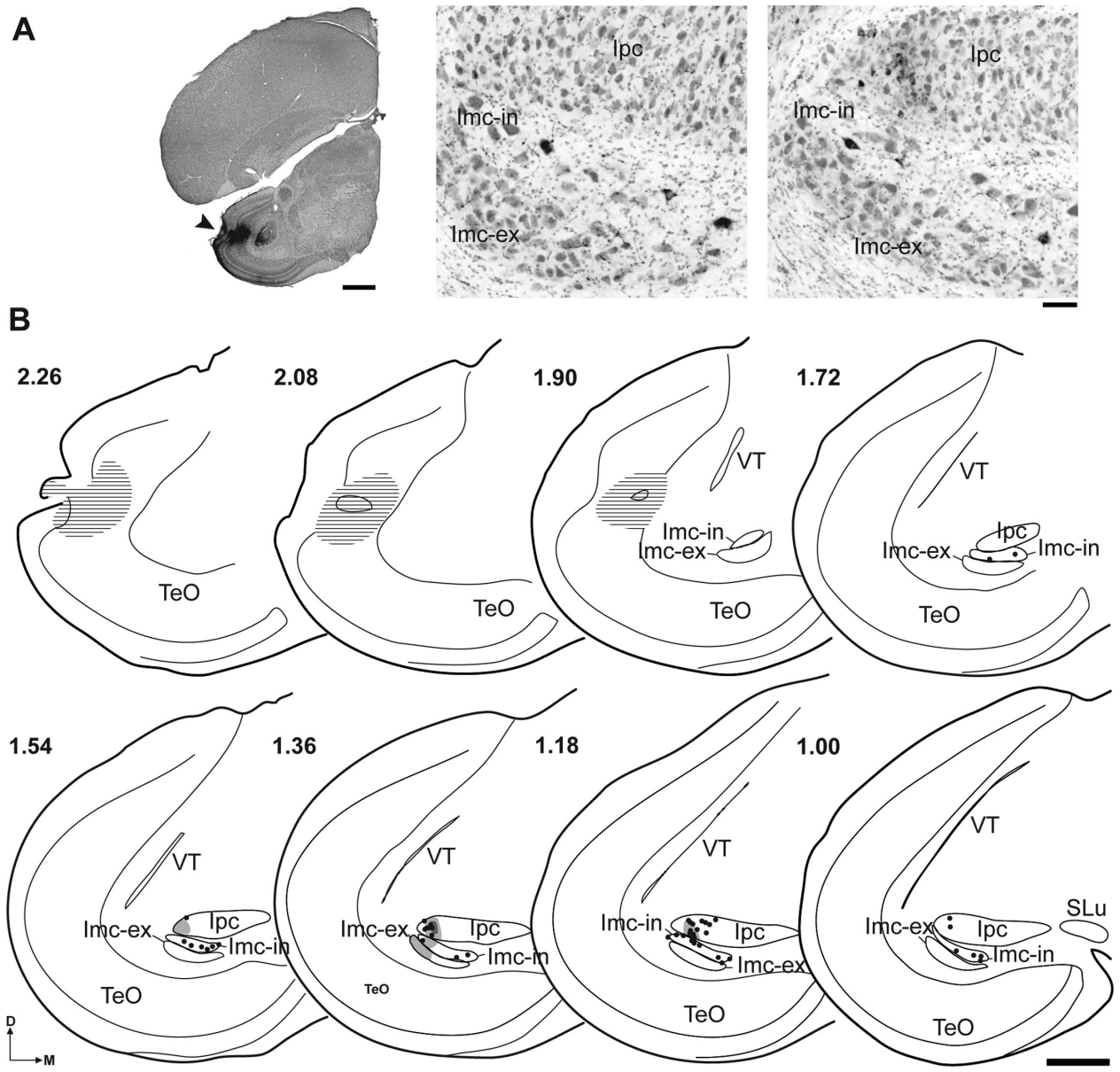


**Figure 6.** Retrogradely labeled cells in the lmc after an in vivo CTB microinjection in the optic tectum. **A**: Brightfield photomicrographs of 60-μm Nissl-counterstained coronal sections containing the injection site in the TeO (arrowhead) and labeled cells in the nucleus isthmi magnocellularis. **B**: Line drawings of a series of sections are separated by 180 μm. Coronal levels according to Nixdorf-Bergweiler and Bischof (2007). Dots represent labeled somata, hatched area represents injected tracer, and light gray shadow represents labeled fibers. For abbreviations, see Figure 1 legend. Scale bar = 200 μm in A, left; 50 μm in A middle and right; 500 μm in B.

Although phylogenetic relationships among avian orders continues to be a highly controversial issue (Fain and Houde, 2004; Harshman, 2007; Livezey and Zusi, 2007; Brown et al., 2008; Pratt et al., 2008), according to recent molecular and morphological phylogenetic analyses, the closest group to passerines is Psittaciformes (Ericson et al., 2006; Hackett et al., 2008; Ksepka et al., 2011; Suh et al., 2011). Passerines and Psittaciformes are both probably related to Falconiformes (Ericson et al., 2006; Hackett et al., 2008; Suh et al., 2011). Moreover, the order Piciformes is grouped inside the paraphyletic clade referred to as "Coraciiformes" (Hackett et al., 2008; Mayr, 2008; Clarke et al., 2009). Thus, our observation of a uniform lmc in two species of the suborder Alcedines ("Coraciformes"), nine species of Psittaciformes, and one species of Falconiformes indicates that a synapomorphy of this trait in Passeriformes and Piciformes is very unlikely. It would require at least three independent losses, and even a fourth one in owls (Strigiformes). Accordingly, we consider that the more parsimonious hypothesis is that the appearance of a segregated lmc occurred in parallel in passerines and piciforms. The appearance of this trait in

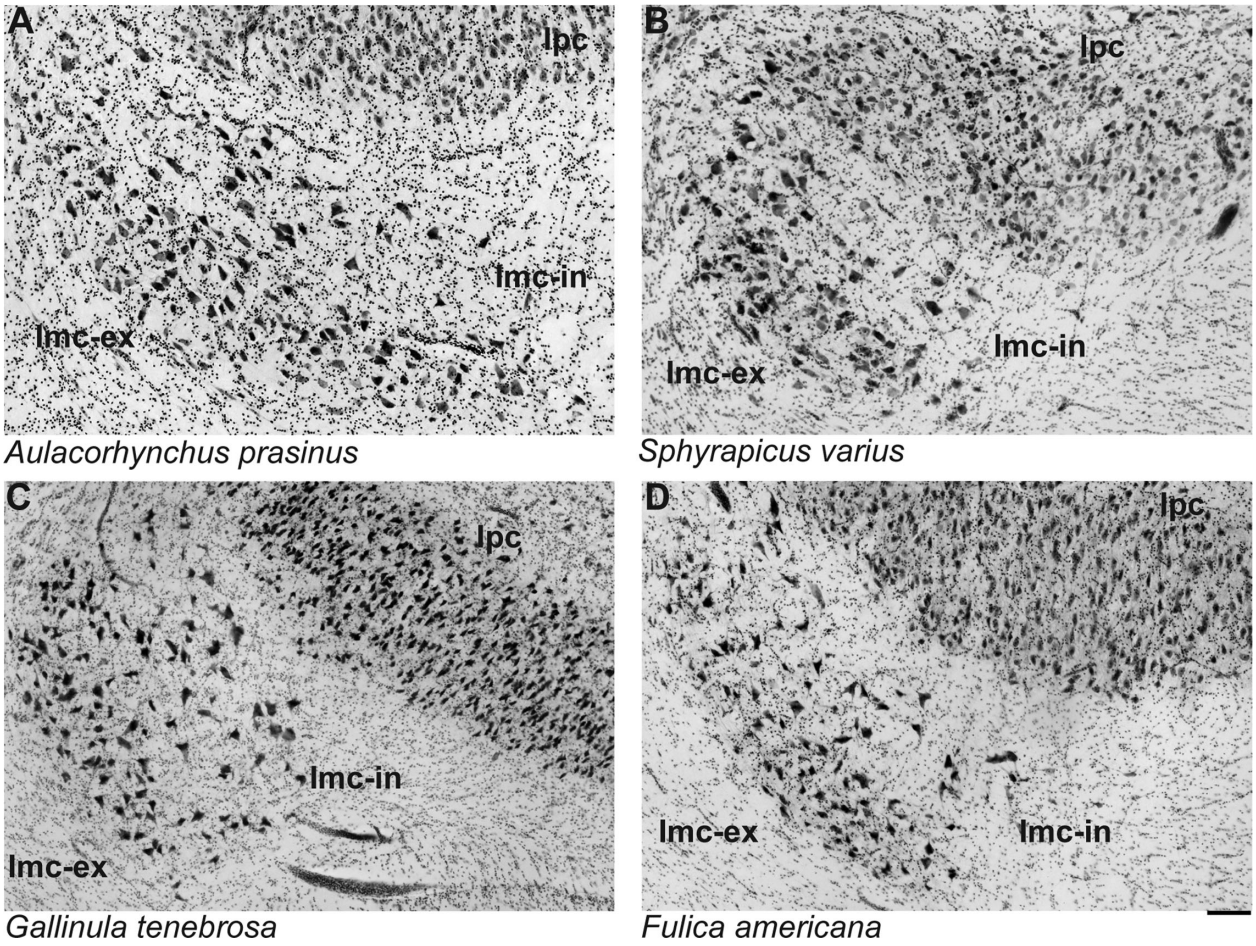


**Figure 7.** Brightfield photomicrographs of 60-μm Nissl-stained coronal sections of the nucleus isthmi magnocellularis in some non-passerine bird species exhibiting a segregated Imc. **A**: The emerald toucanet, *Aulacorhynchus prasinus*, family Ramphastidae, order Piciformes. **B**: The yellow-bellied sapsucker, *Sphyrapicus varius*, family Picidae, order Piciformes. **C**: The dusky moorhen, *Gallinula tenebrosa*, family Rallidae, order Gruiformes. **D**: The american coot, *Fulica americana*, family Rallidae, order Gruiformes. For abbreviations, see legend to Figure 1. Scale bar = 100 μm in D (applies to A–D).

rails suggests a third independent event, given its absence in putatively related groups, such as Pelecaniformes and Procellariformes (Fig. 8).

Thus, this segregation of the two Imc cell types has occurred at least three times in avian evolution, and constitutes a divergence in the organization of the isthmotectal circuit compared with the most common type found in birds. It might reflect a common pattern of specialization in visual function shared by passerines, piciforms, and rails, but based on the ecology and behavior of species within these three taxa, it is difficult to determine what that common function might be.

## Possible functional significances of the Imc segregation

It is hard to visualize a straightforward relationship between the specialization of the isthmotectal network and a specific visual behavior. Indeed, passerines alone exhibit a great variety of visual behaviors (e.g., ground feeding, insect catching, etc.), and rails and piciforms add a wider behavioral diversity of species possessing a segregated Imc.

The bottom-up mechanism of spatial attention (Konig and Luksch, 1998; Knudsen, 2007), in which the Imc nucleus is thought to be involved, is probably an essential component of the tectofugal system. Thus, the specialization of the isthmotectal network could actually reflect an enhanced development of the tectofugal system as a whole. Iwaniuk et al. (2010) compared the relative volumes of some of the components of the tectofugal pathway among several avian orders, finding no significant enlargements of any tectofugal region among the compared groups. However, they suggested that different degrees of specialization might be detected by looking at a more refined level (Iwaniuk et al., 2010). One sign of

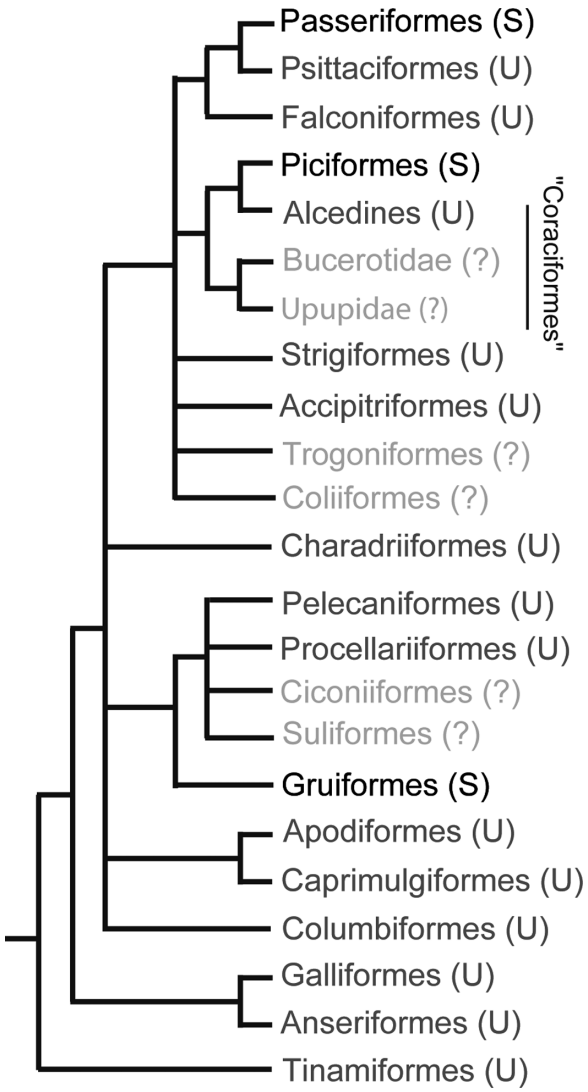


**Figure 8.** The segregation of the avian nucleus isthmi magnocellularis appeared at least three times. Simplified consensus cladogram based on Ericson et al. (2006), Hackett et al. (2008), Mayr (2011), and Suh et al. (2011), following the taxonomic nomenclature from Gill and Donsker (2012). Avian orders with a segregated Imc are written in black (S), those with a uniform Imc in dark gray (U), and those in which the organization of the Imc is unknown (?) are written in light gray.

system specialization is the degree of parcellation of the structures (Ebbesson, 1984), an example of which would be the case presented in this study. Indeed, passerines do appear to have a highly differentiated tectofugal system, as they exhibit a highly sublaminated TeO, and distinct subnuclei in the Rt and entopallium, exceeding the number found in pigeons and chicks (H.J. Karten, unpublished data). The visual system of piciform and rallid birds is still poorly known, so it is unclear whether they share a similarly differentiated tectofugal system to that of passerines.

## Comparison with other diapsids

In turtles, in which the precise anatomy of the isthmotectal network was first elucidated (Sereno and Ulinski, 1987), two isthmic nuclei can be distinguished. On the basis of their homology (hodological and immunohistochemical) to the avian isthmic nuclei, these nuclei are called isthmi pars parvocellularis and isthmi pars magnocellularis (Powers and Reiner, 1993). Serial section reconstructions of axonal and dendritic arborizations of horseradish peroxidase-filled Imc cells revealed that these cells apparently project to both the TeO and the Ipc nucleus (Sereno and Ulinski, 1987). Thus, we can recognize at least three types of Imc nucleus in diapsids: one in which the same cell sends collateral axons to both targets, as in the turtle; a second one in which these two projections originate from different cell populations that are found intermingled within the Imc nucleus (Wang et al., 2004), as in the chick and presumably most non-passerine birds; and finally, a third one in which these two cell populations are spatially segregated as in passerines, and presumably in rails and piciforms (Fig. 9). The organization of the Imc nucleus remains unknown in other diapsid groups, such as crocodiles and lepidosauromorphs, but such information would provide further insight into the evolution of the isthmotectal network among vertebrates.

## The zebra finch as a model system for study of the isthmotectal network

The zebra finch has been extensively used as a model for the study of song learning (Brainard and Doupe, 2002). However, this is the first attempt to use it for investigating the avian isthmotectal network, which has been so far done by using the chick, the pigeon, and the owl.

The Imc nucleus is involved in long-range inhibitory interactions among visually active loci in the Ipc, which would focus the feedback from the Ipc on those tectal locations receiving the strongest visual stimulation. This would result in a bottom-up mechanism for attention and stimulus selection (Marín et al., 2005, 2007, 2012; Mysore et al., 2010, 2011; Asadollahi et al., 2011; Knudsen, 2011). This long-range inhibition could occur in parallel, both in the Ipc and in the SLu, via the Imc-Is neurons, and in the TeO, via the Imc-Te neurons. The spatial segregation of the two Imc cell types poses the question: what role does each cell population play in visual attention and stimulus selection? As the Imc-Te cells only project to deep layers of the TeO (layers 10–12), whereas the Ipc and SLu cells project to both deep and superficial layers (including retino-recipent layers), only the Imc-Is cells would have an effect upon the activity of the superficial (retino-recipient) tectal layers. It is also unknown whether the projection from the Imc to the Ipc is

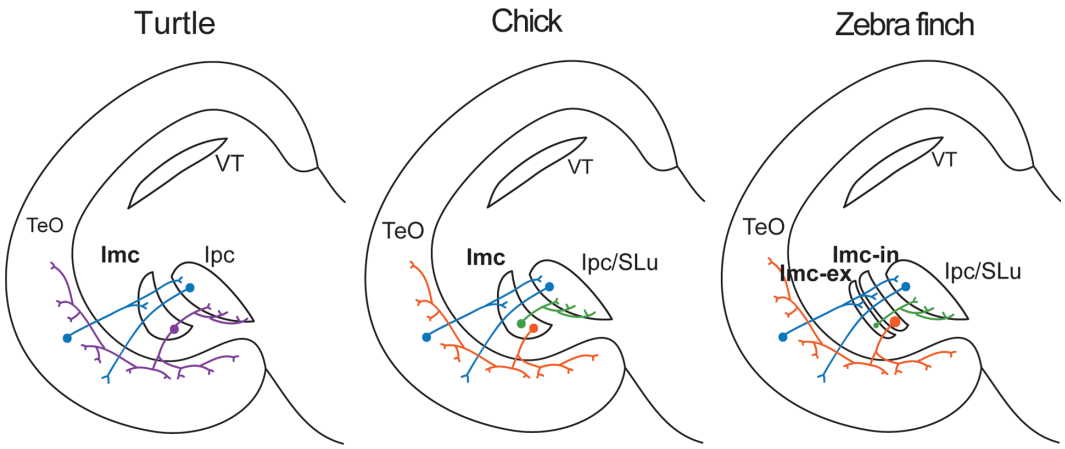


Figure 9. Schematic drawing depicting the three types of nucleus isthmi magnocellularis found in diapsids. In the turtle, the projection to the optic tectum and to the nucleus isthmi parvocellularis originate from collaterals of the same cells (Sereno and Ulinski, 1987); in the chick, as in most non-passerine birds, these projections arise from different cell populations that are found intermingled within the Imc nucleus (Wang et al., 2004; and the present study); and in passerines and presumably in rails and piciforms, these two cell populations are spatially segregated. For abbreviations, see legend to Figure 1.

antitopographic, comparable to the projection upon the TeO. Some models of the circuit operation suggest that antitopography is a key requirement for stimulus selection (Lai et al., 2012). A recent study indicates that mutual inhibition between Imc neurons would allow the circuit to select the strongest stimuli regardless of the absolute strength of the competitors (Mysore and Knudsen, 2012). Although mutual inhibition between Imc neurons has been reported in the chick (Li et al., 2007), it may occur within or across cell types.

In pigeons, the Imc-Is neurons synchronize at high firing frequencies (Marín et al., 2007), either by a synchronized shepherd-crook input or by the coupling of the Imc neurons. It is unknown whether the Imc-Is and Imc-Te cells receive projections from the same population of shepherd-crook neurons (i.e., collaterals of the same neuron), or from two different subpopulations. The parcellation of the Imc suggests that each cell population may receive distinct tectal inputs and act as separate synchronized ensembles, carrying inhibitory waves at different frequencies and/or phases to their respective targets. Perhaps this feat is also accomplished, to a lesser degree, in birds with a uniform Imc nucleus.

Our results point to the zebra finch as an excellent model for the study of this network, allowing the separate examination of the physiology and anatomy of the two cell populations of the avian Imc, necessary for solving pending problems such as their connectivity to the TeO and their physiological role in the network operation.

## ACKNOWLEDGMENTS

We thank Sergio Soto from the Museo Nacional de Historia Natural de Chile for expert advice on avian phylogeny, Verónica Orellana for help with the preparation of the figures, and João Botelho and Pablo Henny for reviewing the manuscript.

## CONFLICT OF INTEREST STATEMENT

The authors declare no conflict of interest that could inappropriately influence or be perceived to influence their work.

## ROLE OF AUTHORS

All authors had full access to all the data in the study and take responsibility for the integrity of the data and the accuracy of the data analysis. Study concept and design: M.F., S.F., C.G.I., A.N.I., D.R.W., J.M., H.J.K., G.M. Acquisition of data: M.F., S.F., C.G.I. Analysis and interpretation of data: M.F., S.F., C.G.I., A.N.I., D.R.W., J.M., H.J.K, G.M. Drafting of the manuscript: M.F., S.F., J.M., G.M. Critical revision of the manuscript for important intellectual content: C.G.I., A.N.I., D.R.W., H.J.K. Statistical analysis: M.F., S.F., C.G.I. Obtained funding: D.R.W., G.M. Administrative, technical, and material support: M.F., S.F., C.G.I., A.N.I., D.R.W., J.M., H.J.K., G.M. Study supervision: G.M.

## LITERATURE CITED

Asadollahi A, Mysore SP, Knudsen EI. 2010. Stimulus-driven competition in a cholinergic midbrain nucleus. Nat Neurosci 13:889–895.

Asadollahi A, Mysore SP, Knudsen EI. 2011. Rules of competitive stimulus selection in a cholinergic isthmic nucleus of the owl midbrain. J Neurosci 31:6088–6997.

Brainard MS, Doupe AJ. 2002. What songbirds teach us about learning. Nature 417:351–358.

Braun K, Scheich H, Zuschratter W, Heizmann CW, Matute C, Streit P. 1988. Postnatal development of parvalbumin-,

calbindin- and adult GABA-immunoreactivity in two visual nuclei of zebra finches. Brain Res 475:205–217.
Brown JW, Rest JS, Garcia-Moreno J, Sorenson MD, Mindell DP. 2008. Strong mitochondrial DNA support for a Cretaceous origin of modern avian lineages. BMC Biol 6:6.
Clarke JA, Ksepka DT, Smith NA, Norell M. 2009. Combined phylogenetic analysis of a new North American fossil species confirms widespread Eocene distribution for stem rollers (Aves, Coracii). Zool J Linnean Soc 157:586–611.
Domenici L, Waldvogel HJ, Matute C, Streit P. 1988. Distribution of GABA-like immunoreactivity in the pigeon brain. Neuroscience 25:931–950.
Ebbesson SOE. 1984. Evolution and ontogeny of neural circuits. Behav Brain Sci 7:321–366.
Ericson PGP, Christidis L, Irestedt M, Norman JA. 2002. Systematic affinities of the lyrebirds (Passeriformes: Menura), with a novel classification of the major groups of passerine birds. Mol Phylogenet Evol 25:53–62.
Ericson PGP, Anderson CL, Ohlson JI, Parsons TJ, Zuccon D, Mayr G. 2006. Diversification of Neoaves: integration of molecular sequence data and fossils. Biol Lett 2: 543–547.
Fain MG, Houde P. 2004. Parallel radiations in the primary clades of birds. Evolution 58:2558–2573.
Gill F, Donsker D. 2012. IOC World Bird Names (v 3.1). Available from: http://www.worldbirdnames.org.
Gruberg E, Dudkin E, Wang Y, Marín G, Salas C, Sentis E, Letelier J, Mpodozis J, Malpeli J, Cui H, Ma R, Northmore D, Udin S. 2006. Influencing and interpreting visual input: the role of a visual feedback system. J Neurosci 26: 10368–10371.
Güntürkün O, Remy M. 1990. The topographical projection of the nucleus isthmi pars parvocellularis (Ipc) onto the tectum opticum in the pigeon. Neurosci Lett 111:18–22
Hackett SJ, Kimball RT, Reddy S, Bowie RCK, Braun EL, Braun MJ, Chojnowski JL, Cox WA, Han K-L, Harshman J, Huddleston J, Marks BD, Miglia KJ, Moore WS, Sheldon FH, Steadman DW, Witt CC, Yuri T. 2008. A phylogenomic study of birds reveals their evolutionary history. Science 320:1763–1768.
Harshman J, 2007. Classification and phylogeny of birds. In: Jamieson BGM, editor. Reproductive biology and phylogeny of birds. Enfield, NH: Science Publishers. p 1–35.
Hunt SP, Streit P, Künzle H, Cuénod M. 1977. Characterization of the pigeon isthmo-tectal pathway by selective uptake and retrograde movement of radioactive compounds and by Golgi-like horseradish peroxidase labeling. Brain Res 129:197–212.
Iwaniuk AN, Gutiéerrez-Ibáñez C, Pakan JMP, Wylie DR. 2010. Allometric scaling of the tectofugal pathway in birds. Brain Behav Evol 2010:122–137.
Knudsen EI. 2007. Fundamental components of attention. Annu Rev Neurosci 30:57–78.
Knudsen EI. 2011. Control from below: the role of a midbrain network in spatial attention. Eur J Neurosci 33:1961–1972.
Konig P, Luksch H. 1998. Active sensing—closing multiple loops. Z Naturforsch 53:542–549.
Ksepka DT, Clarke JA, Grande L. 2011. Stem parrots (Aves, Halcyornithidae) from the Green River formation and a combined phylogeny of Pan-Psittaciformes. J Paleontol 85: 835–852.
Lai D, Brandt S, Luksch H, Wessel R. 2011. Recurrent antitopographic inhibition mediates competitive stimulus selection in an attention network. J Neurophysiol 105: 793–805.
Li D-P, Xiao Q, Wang S-R. 2007. Feedforward construction of the receptive field and orientation selectivity of visual neurons in the pigeon. Cereb Cortex 17:885–893.
Livezey BC, Zusi RL. 2007. Higher-order phylogeny of modern birds (Theropoda, Aves: Neornithes) based on comparative anatomy. II. Analysis and discussion. Zool J Linnean Soc 149:1–95.
Maczko K, Knudsen PF, Knudsen EI. 2006. Auditory and visual space maps in the cholinergic nucleus isthmi pars parvocellularis of the barn owl. J Neurosci 26:12799–806.
Marín G, Mpdozis J, Sentis E, Ossandón T, Letelier JC. 2005. Oscillatory bursts in the optic tectum of birds represent re-entrant signals from the nucleus isthmi pars parvocellularis. J Neurosci 25:7081–7089.
Marín G, Salas C, Sentis E, Rojas X, Letelier JC, Mpodozis J. 2007. A cholinergic gating mechanism controlled by competitive interactions in the optic tectum of the pigeon. J Neurosci 27:8112–8121.
Marín GJ, Duran E, Morales C, González-Cabrera C, Sentis E, Mpodozis J, Letelier JC. 2012. Attentional capture? Synchronized feedback signals from the isthmi boost retinal signals to higher visual areas. J Neurosci 32: 1110–1122.
Mayr G. 2008. Avian higher-level phylogeny: well-supported clades and what we can learn from a phylogenetic analysis of 2954 morphological characters. J Zool System Evol Res 46:63–72.
Mayr G. 2011. Metaves, Mirandornithes, Strisores and other novelties—a critical review of the higher-level phylogeny of neornithine birds. J Zool System Evol Res 49:58–76.
Medina L, Reiner A. 1994. Distribution of choline acetyltransferase immunoreactivity in the pigeon brain. J Comp Neurol 342:497–537.
Meyer U, Shao J, Chakrabarty S, Brandt SF, Luksch H, Wessel R. 2008. Distributed delays stabilize neural feedback systems. Biol Cybernet 99:79–87.
Mikula S, Trotts I, Stone JM, Jones EG. 2007. Internet-enabled high-resolution brain mapping and virtual microscopy. NeuroImage 35:9–15. Available from: http://brainmaps.org.
Mysore SP, Knudsen EI. 2012. Reciprocal inhibition of inhibition: a circuit motif for flexible categorization in stimulus selection. Neuron 73:193–205.
Mysore SP, Asadollahi A, Knudsen EI. 2010. Global inhibition and stimulus competition in the owl optic tectum. J Neurosci 30:1727–1738.
Mysore SP, Asadollahi A, Knudsen EI. 2011. Signaling of the strongest stimulus in the owl optic tectum. J Neurosci 31: 5186–5196.
Nixdorf-Bergweiler B, Bischof H. 2007. A stereotaxic atlas of the brain of the zebra finch, *Taeniopygia guttata*: with special emphasis on telencephalic visual and song system nuclei in transverse and sagittal sections. Bethesda, MD: National Center for Biotechnology Information.
Powers AS, Reiner A. 1993. The distribution of cholinergic neurons in the central nervous system of turtles. Brain Behav Evol 41:326–345.
Pratt RC, Gibb GC, Morgan-Richards M, Phillips MJ, Hendy MD, Penny D. 2008. Toward resolving deep Neoaves phylogeny: data, signal enhancement, and priors. Mol Biol Evol 26:313–326.
Sereno MI, Ulinski PS. 1987. Caudal topographic nucleus isthmi and the rostra1 nontopographic nucleus isthmi in the turtle, *Pseudemys scriptu*. J Comp Neurol 346:319–346.
Shao J, Lai D, Meyer U, Luksch H, Wessel R. 2009. Generating oscillatory bursts from a network of regular spiking neurons without inhibition. J Comput Neurosci 27: 591–606.
Suh A, Paus M, Kiefman M, Churakov G, Franke FA, Brosius J, Kriegs JO, Schmitz J. 2011. Mesozoic retroposons reveal parrots as the closest living relatives of passerine birds. Nat Commun 2:443.

Sun Z, Wang HB, Laverghetta a, Yamamoto K, Reiner A. 2005. The distribution and cellular localization of glutamic acid decarboxylase-65 (GAD65) mRNA in the forebrain and midbrain of domestic chick. J Chem Neuroanat 29:265–81.

Tömböl T, Németh A. 1998. GABA-immunohistological observations, at the electron-microscopical level, of the neurons of isthmic nuclei in chicken, *Gallus domesticus*. Cell Tissue Res 291:255–266.

Wang Y, Major DE, Karten HJ. 2004. Morphology and connections of nucleus isthmi pars magnocellularis in chicks (*Gallus gallus*). J Comp Neurol 469:275–297.

Wang Y, Luksch H, Brecha NC, Karten HJ. 2006. Columnar projections from the cholinergic nucleus isthmi to the optic tectum in chicks (*Gallus gallus*): a possible substrate for synchronizing tectal channels. J Comp Neurol 494: 7–35.